Effect of Strain Rate on the Flow Stress of Three Liquid Phase Sintered Tungsten Alloys

R. L. WOODWARD, N. J. BALDWIN, I. BURCH, and B. J. BAXTER

Stress/strain tests were carried out in compression on three liquid phase sintered tungsten alloys, with tungsten contents of 90, 95, and 97.4 wt pct, in the strain rate range 10^{-3} s^{-1} to 10^{3} s^{-1}. Each alloy shows a gradual increase of flow stress with strain rate, and evidence of work softening is observed when the strain rate is of the order of 2 s^{-1} or greater. The work softening effect is shown to result from a temperature rise due to the plastic deformation and partly masks the strain rate effect at strains greater than 0.1. The 97.4 pct tungsten alloy also shows variable behavior due to cracking associated with the presence of a brittle phase at the tungsten particle/matrix interface.

I. INTRODUCTION

MOST metals exhibit an increase in flow stress as the strain rate is increased, and extensive examinations of strain rate effects in many individual alloy systems have been undertaken with results summarized in a number of reviews.[1-4] Liquid phase sintered tungsten alloys are a recent development and only a small amount of information is available on the effect of strain rate on strength.[5,6,7] The deformation and fracture behavior in these alloys is not fully understood and the contribution of minor phases to intergranular failure is the subject of considerable research effort.[8,9] In this work the flow stresses of three tungsten alloys are examined over a large range of strain rates, 10^{-3} s^{-1} to 10^{3} s^{-1}, and the nature of the stress/strain behavior is interpreted in terms of the testing conditions, thermomechanical characteristics, and microstructure.

II. CHARACTERIZATION OF MATERIALS

The alloys used in this study are designated as 90WNiCu, 95WNiFe, and 97WNiFeCu, respectively, where the numeral represents the nominal weight percentage of tungsten (W) in the alloy and the other symbols indicate the principal alloying elements. The materials are composed of spheroidal grains of nearly pure tungsten surrounded by a binder phase, which is a solid solution of tungsten with the alloying elements. Typical microstructures (Figure 1) show the differences in grain sizes, grain shapes, and volume fractions of tungsten and binder phase among the three alloys. Table I lists compositions, both nominal and obtained by chemical analysis of the test materials, and also electron probe microanalysis results for the binder phase in each alloy and for a brittle phase which was observed in the 97WNiFeCu alloy. X-ray diffraction was carried out to determine the structure of the binder phase, which was found to be face-centered cubic with a lattice parameter of 0.358 nm for all alloys. Physical property data for the alloys are given in Table II.

All the alloys were tested in the as-received condition. Following its sintering treatment the 95WNiFe alloy had been subjected to a vacuum anneal at 1100 °C followed by rapid cooling. The 97WNiFeCu alloy was in the as-sintered condition, but no information was available on whether the 90WNiCu had received any post sintering heat treatment.

III. TESTING PROCEDURE

Compression tests were carried out on 4.76 mm nominal diameter cylinders with a height-to-diameter ratio of one. This is a compromise which avoids the problems of buckling at larger height-to-diameter ratios, and friction effects which occur at low height-to-diameter ratios. A thin layer of teflon was used to minimize frictional constraint with the platen ends; however, slight barrelling was observed with some evidence of nonuniform deformation in sectioned samples. Earlier work[10] indicates that the effect of friction on the flow stress values under these test conditions will be less than the scatter of materials properties observed in the present tests; thus, as the tests are all performed in the same manner and are comparative, no correction is made for friction effects. The load and platen positions were monitored continuously during the tests and the true stress and true strain calculated.

To obtain a range of strain rates, three testing machines were used. A screw testing machine provided strain rates in the range 10^{-3} s^{-1} to 10^{-1} s^{-1}. A servo-hydraulic machine used in stroke control allowed strain rates from 10^{-1} s^{-1} to 15 s^{-1} to be achieved, and a drop weight machine gave rates in the range 2×10^{2} s^{-1} to 10^{3} s^{-1}. On both the screw testing machine and the hydraulic machine tungsten carbide platens were used; however, it was necessary to use hardened steel platens on the drop weight tester for impact toughness. Transducers mounted close to the sample were used to measure displacement. On the drop weight machine, a fiber optic probe was used to measure the distance between the platens by recording variations in reflected light intensity with distance. This system required calibration at regular intervals. The drop weight tester incorporated a piezoelectric load cell and was designed so that the amount of deformation could be restricted to a preset amount by the use of spacers. The arrangement of platens and transducers in the drop weight tester is shown schematically in Figure 2. The lower limit on strain rate with the drop weight tester was determined by the mass which limited the amount of kinetic energy that could be obtained with small drop heights. For each machine, the testing was at approximately constant

R. L. WOODWARD, N. J. BALDWIN, I. BURCH, and B. J. BAXTER are with the Australian Department of Defence, Materials Research Laboratories, P.O. Box 50, Ascot Vale, 3032, Victoria, Australia.

Manuscript submitted December 4, 1984.

Table I. Alloy and Phase Composition

Alloy	Phase	Element, Weight Percent					
		W	Ni	Fe	Cu	Co	Si
90WNiCu	nominal alloy	90.0	7.5		2.5		
	alloy analysis	bal	6.2	0.6	2.3		
	binder phase	22.8	60.0		17.1		
95WNiFe	nominal alloy	95.0	3.5	1.5			
	alloy analysis	bal	3.6	1.5			
	binder phase	23.4	55.3	21.4			
97WNiFeCu	nominal alloy	97.4	(2.6-Ni, Fe, Cu)				
	alloy analysis	bal	1.3	0.6	0.3	trace	
	binder phase	7.8	47.8	19.5	18.5	2.9	3.5
	brittle phase	68.2	17.2	7.2		2.2	5.2

Table II. Physical Properties of the Alloys

Alloy	Hardness (HV10)	Density (kg m^{-3})	Tensile Elongations (at 10^{-3} s^{-1})
90 WNiCu	323	17.1×10^{-3}	3 pct to 8 pct
95 WNiFe	320	18.0×10^{3}	15 pct to 30 pct
97 WNiFeCu	305	18.6×10^{3}	0 pct to 5 pct

velocity, and the strain rate quoted is the mean value obtained by dividing the total strain in the sample by the time of the test.

The force/time response from the piezo-electric transducer in the drop weight machine included high frequency oscillations. Similar behavior has been observed in other cases[11,12,13] and as with Lindholm *et al.*[11] a mean line was drawn through the oscillations. This is justified in the Appendix by examining the response of a second order spring-mass-dashpot system.

IV. RESULTS AND DISCUSSION

The results of stress/strain tests are presented in two forms, *viz.*, typical stress/strain curves at a range of strain rates for the three alloys (Figure 3), and plots of flow stress as a function of strain rate for four levels of strain (Figure 4). The typical stress/strain curves of Figure 3 should be used as a guide to the shape of the curve, keeping in mind that Figure 4 shows that changes in strength with strain rate while clearly evident are of the same order as the scatter in observed properties. Figure 3 shows that at low strain rates the flow stress increases continuously with strain, but at strain rates in the range 2 s^{-1} to 10 s^{-1} a negative slope appears in the stress/strain curves at a strain of about 0.2. This latter effect appeared for the three alloys in the same strain rate range. Additionally, the 97WNiFeCu alloy showed some curves with negative strain hardening at lower strain rates, and two such curves are shown by dashed lines in Figure 3(c); these results are attributable to fracture effects, discussed later, in some samples and they were therefore not included in the data of Figure 4. Figure 4 shows that the strength levels are similar in the three alloys, and the large number of tests allows the degree of scatter in material properties to be assessed. The effect of strain rate is evident as a gradual increase in flow stress at strains of 0.05 and 0.1, while the effect is not as clear at a strain of 0.2 and a decrease in flow stress with increasing strain rate is seen for strain level 0.4. This decrease in flow stress with increase in strain rate is particularly noticeable as a change at a strain rate of about 1 s^{-1} in Figure 4(d), correlating with the work softening observations made for Figure 3 above. For both the 95WNiFe and the 97WNiFeCu alloys (Figures 4(a), (b), and (c)), an increase in flow stress at a strain rate of about 10 s^{-1} is also indicated.

A gradual increase in flow stress with strain rate is as expected,[2,3,4] but the softening at the higher strain rates needs explanation. Possible causes are cracking, changes in platen friction conditions, nonuniform deformation effects, a yield point, or thermal softening. Cracking at the edge of tungsten alloy compression test pieces has been observed previously;[13] however, in the present tests, it was only a minor phenomenon for both the 90WNiCu and 95WNiFe alloys and was less noticeable at the higher strain rates where the softening was observed. In the 97WNiFeCu alloy more cracking was observed and is described in more detail below; however, this did not explain the general work softening behavior, but rather the variability in properties for this particular alloy.

The contact surfaces of the compressed samples were examined as a function of strain rate and showed no evidence of changes. Furthermore, micrographs of sectioned samples which did and did not exhibit the work softening effect were examined and although some nonuniformity in strain, as described by Papirno *et al.*,[14] was seen in all specimens, no significant change with strain rate was evident. Hence, friction and nonuniform deformation aspects were ruled out as possible causes of the work softening effect.

It is possible for a yield point phenomenon to result in a dropping flow stress with increasing strain and depending on the stiffness of the testing machine, this drop can be rapid or gradual.[12,15,16] A yield point can, however, be removed by prestraining. Specimens prestrained up to a strain of 0.2 in the present experiments still showed the softening effect when retested at the higher strain rates. Hence, a yield point effect was ruled out.

The other possibility, thermal softening, can be tested by calculation and also by the use of incremental tests. Approximate calculations were performed by assuming linear

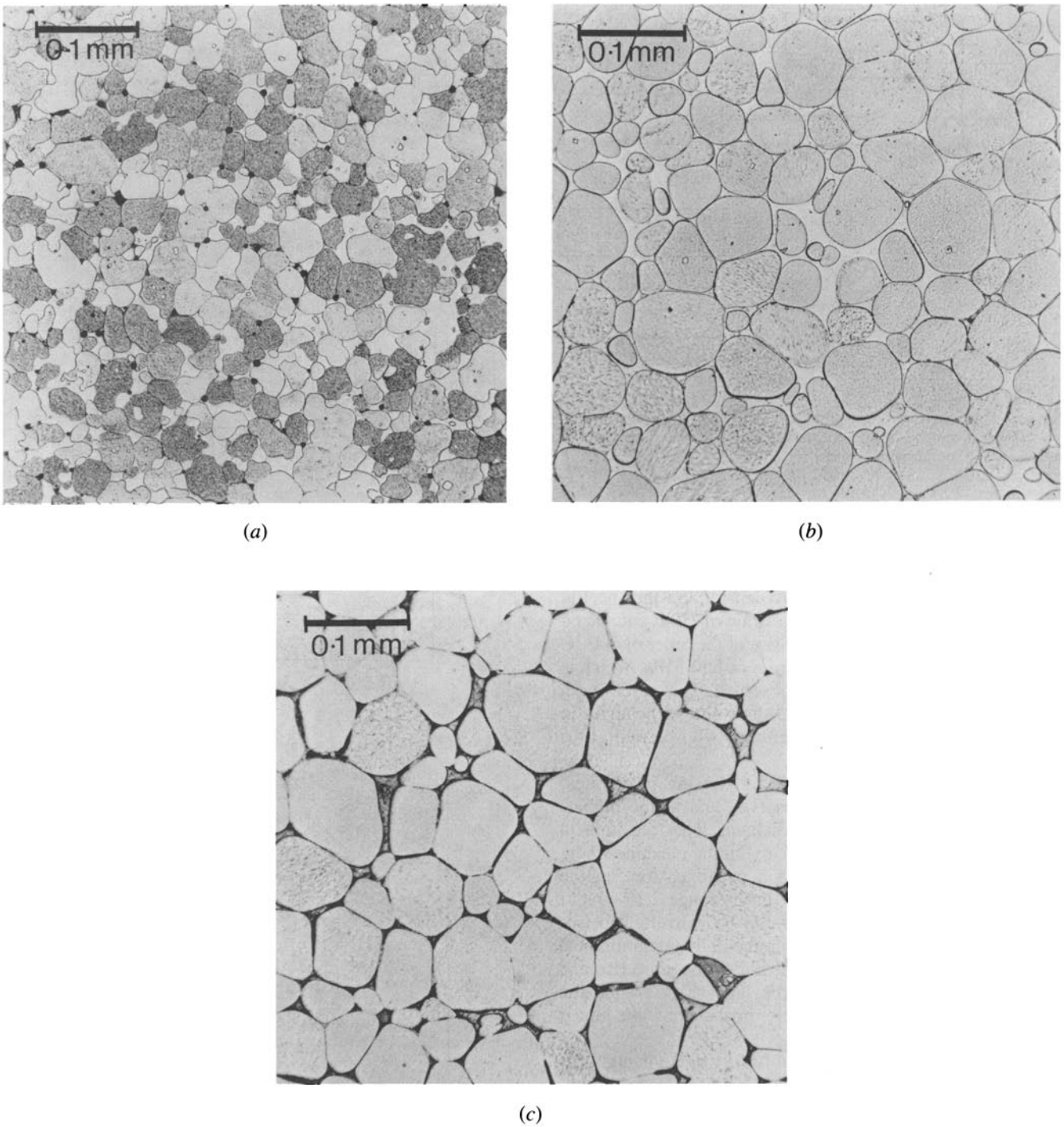

(*a*) (*b*) (*c*)

Fig. 1—Micrographs of the three alloys etched in Murakami's etch. (*a*) 90WNiCu alloy, (*b*) 95WNiFe alloy, and (*c*) 97WNiFeCu alloy.

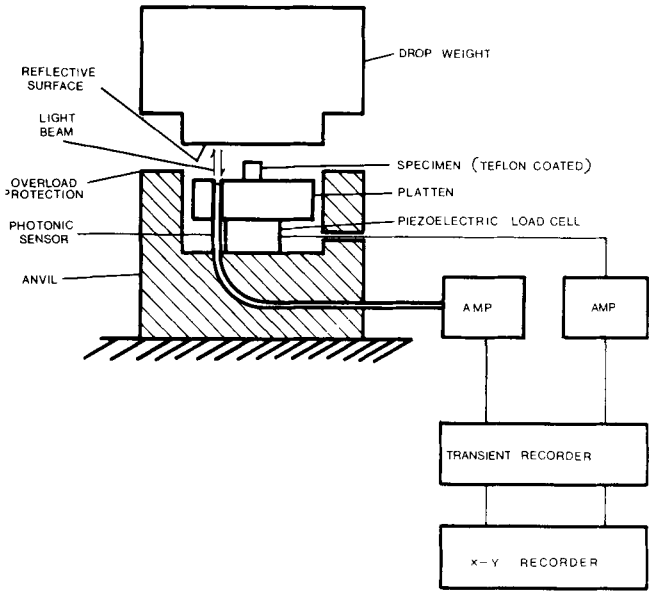

Fig. 2—Schematic drawing of the drop weight testing arrangement to show the positioning of the load cell and the fiber-optic displacement sensor relative to the specimen and platens.

softening of the tungsten alloys between ambient temperature and the liquid phase sintering temperature of the 95WNiFe alloy (1470 °C), and allowing all the plastic work to appear as heat. Using the alloy density and the specific heat of tungsten, compression to a strain of 1.0 is calculated to result in a uniform temperature rise of the order of 600 °C and a drop in flow stress of the order of 650 MPa, which is close to the degree of softening observed. This agrees with the results of Johnson *et al.*,[5] who show similar behavior in dynamic torsion tests on tungsten and who carried out a similar computation.

In the present case, it appears that at very low strain rates, isothermal behavior is being observed and at the highest rates, the tests are effectively adiabatic. The transition in behavior is seen in the tests on the hydraulic machine where softening becomes noticeable as a negative slope in the stress/strain curve at strain rates in the range 2 to 10 s^{-1}. The high speed adiabatic curves can be converted to isothermal stress/strain curves by incrementally integrating the curve, calculating the work done, the temperature rise and stress decrement, then adding the latter to the adiabatic curve. The method is only approximate using the linear softening assumption above.

To investigate the phenomenon further, incremental tests were carried out at strain rates in the critical range to observe the softening with the 95WNiFe alloy. In one case, a specimen was strained in four incremental amounts of 0.15 strain with 5 minutes cooling in alcohol between each increment; work softening was observed and there was a large jump in flow stress associated with the interruptions in the test. In another test, a sample was strained in two incremental amounts of 0.35, again with five minutes cooling in alcohol between increments, so that work softening was again observed. The time at rest again allowed the flow stress to return to a higher value. These results are compared with a

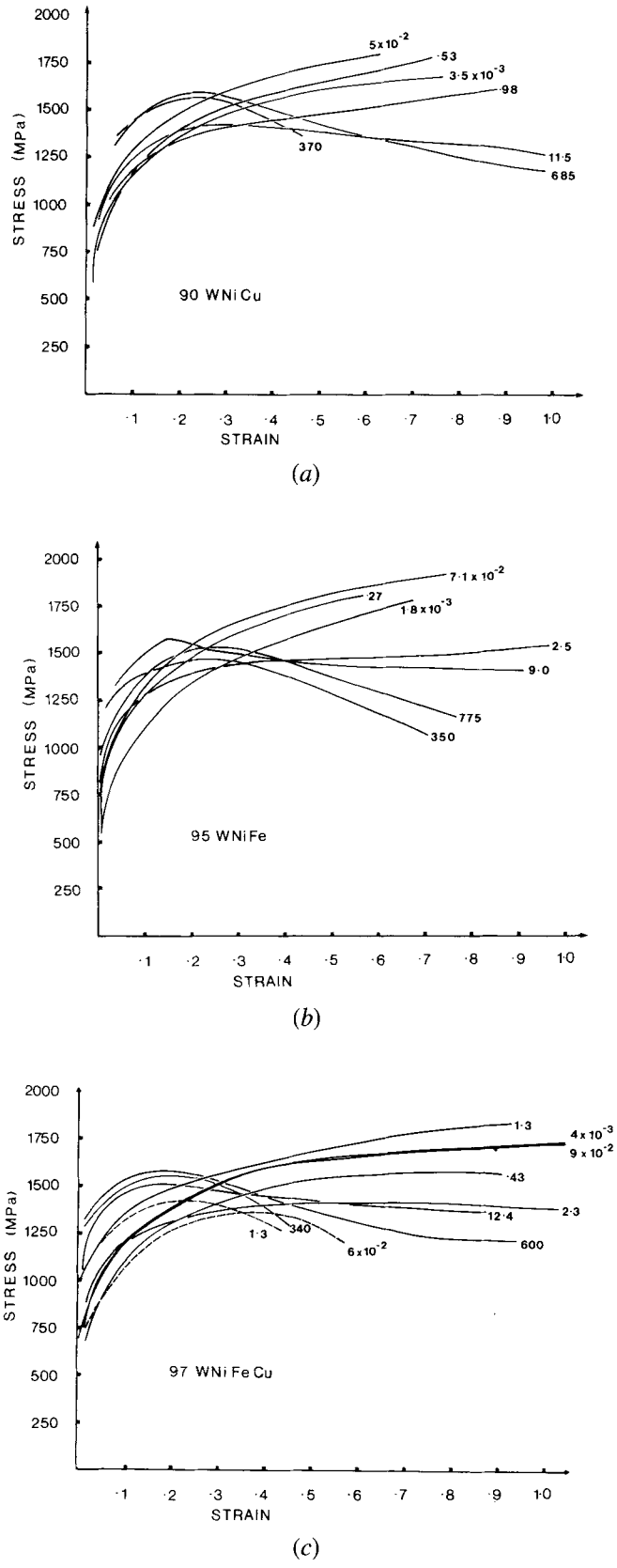

Fig. 3—Typical stress/strain curves at a range of strain rates for each alloy (*a*) 90WNiCu, (*b*) 95WNiFe, and (*c*) 97WNiFeCu. Also shown in (c) are two dashed curves which are typical of some samples which were observed to show brittle behavior in this alloy. Strain rates are indicated on the graphs.

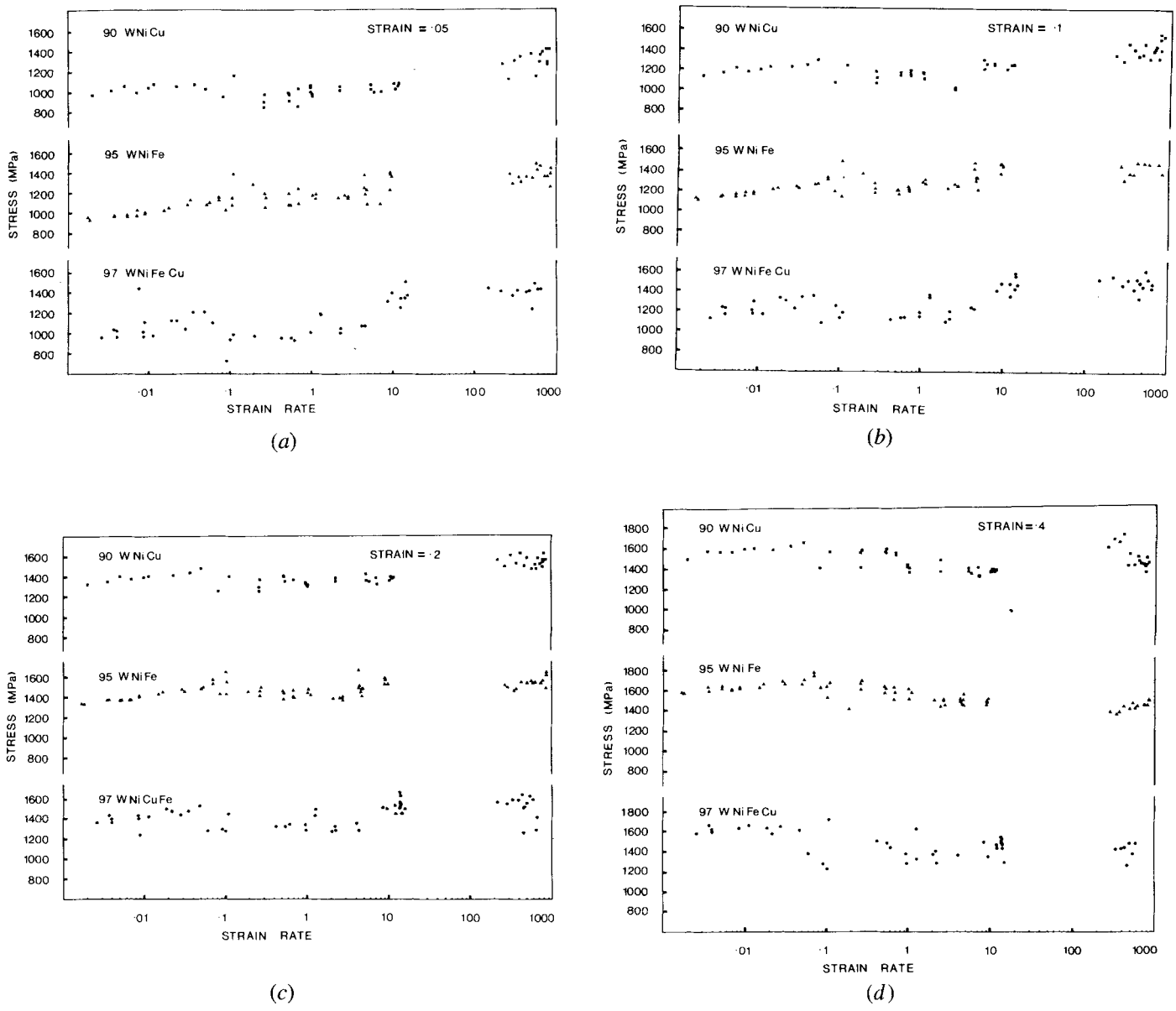

Fig. 4—Plots of stress as a function of strain rate for each alloy, as indicated, at strain levels of (*a*) 0.05, (*b*) 0.1, (*c*) 0.2, and (*d*) 0.4.

continuously strained sample in Figure 5. By drawing a line through the peak flow stress values of the incremental curves, it is clear that thermal softening has played a major role in masking the real strain rate effect in Figures 3 and 4.

The 97WNiFeCu alloy showed variable ductility in the compression tests. At all strain rates some specimens showed extensive cracking and even crumbling in some cases, the proportion of samples showing this behavior increasing with increasing strain rate. In such cases, the load/displacement curves exhibited irregular variations in load and negative slopes followed by a rapid drop to a low load. Typical stress/strain curves for such cases are shown dashed in Figure 3(c) for comparison with results at similar strain rates where the brittle behavior was not observed. Metallographic examination showed that cracking initiated in a brittle phase which occurred at the tungsten particle/matrix interface, as shown in Figure 6, which has been identified in earlier work.[7] The brittle nature of this phase was also evident from extensive cracking in scanning electron microscope observations. The composition of this phase was measured by electron probe microanalysis and is given in Table I. Penrice[7] has indicated that the phase can be removed by a post sintering heat treatment.

V. CONCLUSIONS

Three tungsten alloys were tested to obtain stress/strain curves over a very broad range of strain rates, 10^{-3} to 10^{3} s^{-1}, and it has been shown that, in general, flow stress increases slowly as strain rate increases. Above a strain rate of about 2 s^{-1} work softening occurs in each alloy, due to

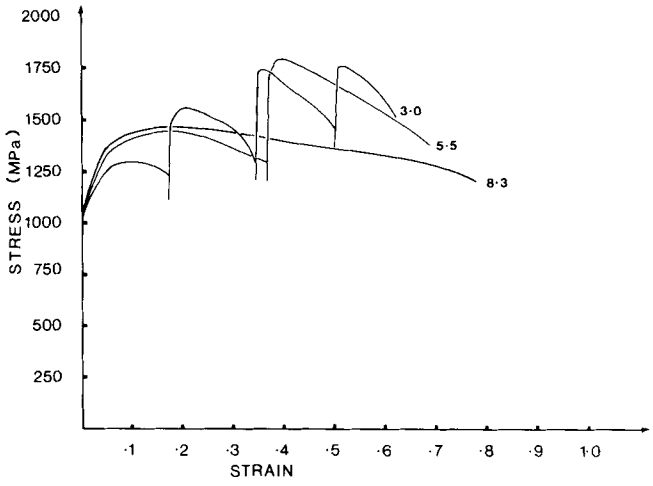

Fig. 5—Plots of stress *vs* strain at strain rates 8.3, 5.5, and 3.0 s^{-1} indicated on the curves, for a continuously compressed specimen, a specimen incrementally compressed with strain increments of 0.15 and allowed to cool between increments, and a specimen compressed in increments of 0.35 strain and allowed to cool between increments. The 95WNiFe alloy was used.

heat generated by plastic flow, and this masks the strain rate effect at strains greater than 0.1 in continuous tests. In addition, variable stress/strain behavior was observed in the alloy 97WNiFeCu, and this is shown to be due to cracking in a brittle phase occurring at the tungsten particle-binder phase interface.

APPENDIX I

Examination of the frequency response of the drop weight testing system

The drop weight testing system employed a piezoelectric force transducer type PCB model 205A with a resonant frequency of 20 kHz. The force displacement graphs show oscillations at a frequency of approximately 9.3 kHz which are damped out with time. Lindholm *et al.*[11] showed similar behavior using a torsion machine and demonstrated that a finite element simulation of the system could reasonably reproduce the oscillations and that a mean line through the oscillations was a satisfactory description of the specimen characteristics. Holzer[12] has argued that such behavior can be modeled as a second order spring-mass-dashpot system. A simulation was therefore performed using Holzer's[12] suggestion to demonstrate that such a model could reproduce the machine response and to see if a mean line through the oscillations was satisfactory.

Cylinders of 5083 aluminum alloy were precompressed slightly and then subjected to both low strain rate tests to determine the stress/strain characteristics, and to drop weight tests to get a load time response of the system. The aluminum alloy was chosen because it is relatively strain rate insensitive, and the precompression ensured a sharp yield so that a clear set of oscillations would be evident in the drop weight test. The output of the transducer as a function of time is shown in Figure A1 for the drop weight test. The system was modeled as shown in the insert of Figure A2 and the equations solved on a digital computer to

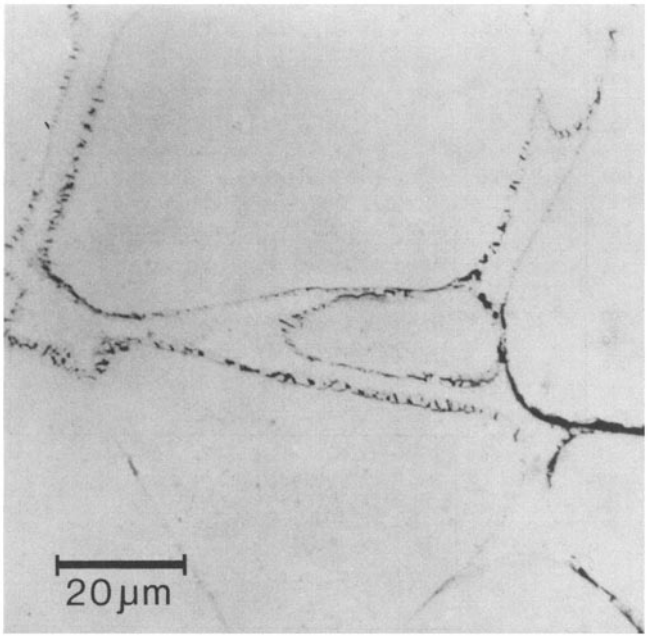

Fig. 6—Unetched sample of the 97WNiFeCu alloy which behaved in a brittle manner, showing the brittle phase evident at the tungsten particle/matrix interface.

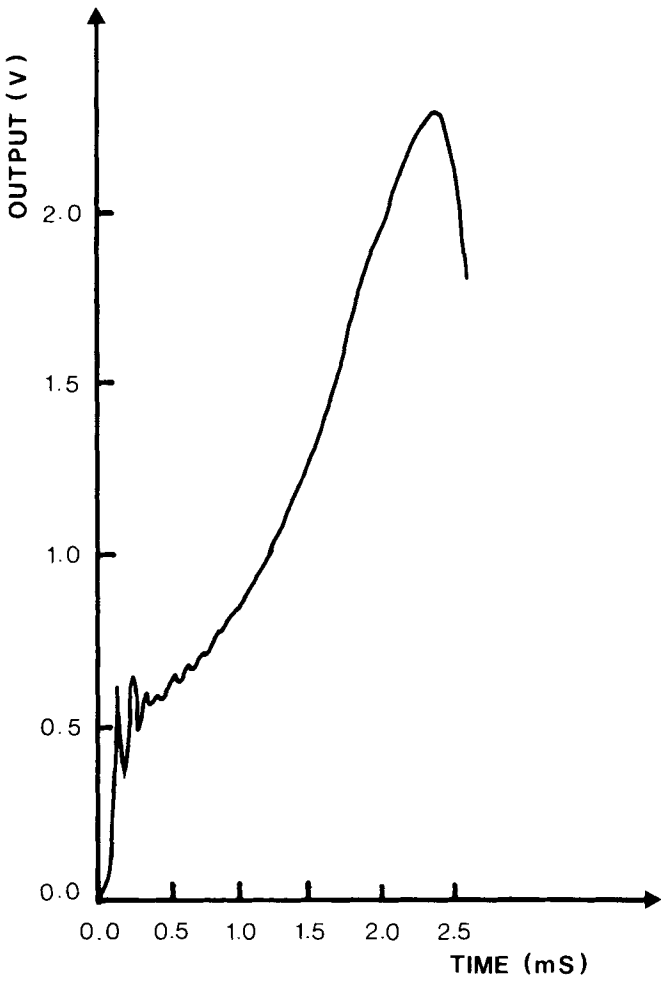

Fig. A1—Output time response of the piezoelectric transducer in the drop weight machine using an aluminum alloy test specimen to show the oscillations at early times.

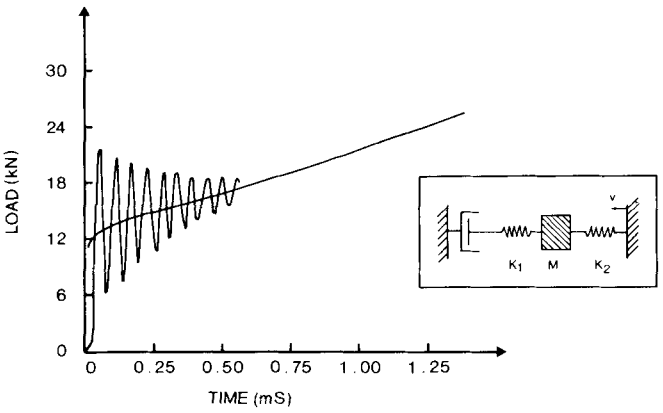

Fig. A2 — Simulated response of the above test showing load as a function of time for the output of the transducer, oscillating curve, and for the load in the specimen, smooth curve. The insert shows the model used in the simulation.

obtain the system response with time. The mass, M, was the combined mass of the load cell and platen in the drop weight tester, the load cell nominal stiffness was used for the spring constant K_1, and the load displacement characteristic of the aluminum sample from the low speed test was used for K_2. The platen was driven at a constant velocity of 1.73 ms^{-1}, and both the load in the load cell and that in the sample are plotted as functions of time in Figure A2. The frequency of the oscillations was 18.5 kHz which is higher than in the test (Figure A1), as is to be expected without knowing the response characteristic of the assembled system; the damping is arbitrarily adjusted as this does not influence the conclusion. The response is of the correct form and the specimen characteristic is very close to a mean line through the oscillations, thus confirming the acceptability of the method.

ACKNOWLEDGMENTS

The authors wish to acknowledge the assistance of Ms. A. Powell who carried out most of the stress/strain calculations and Mr. I. MacDonald and Mr. A. Gunner who performed the chemical and electron probe analyses, respectively.

REFERENCES

1. A. J. Holzer: *Trans. ASME J. Engng. Mats. & Tech.*, 1979, vol. 101, p. 231.
2. K. Bitans and P. W. Whitton: *Int. Met. Rev.*, 1972, vol. 17, p. 66.
3. J. D. Campbell: *Mats. Sci. & Engng.*, 1973, vol. 12, p. 3.
4. J. Duffy: "The Dynamic Plastic Deformation of Metals: A Review", Air Force Wright Aeronautical Laboratories Technical Report, AFWAL-TR-82-4024, Oct. 1982.
5. G. R. Johnson, J. M. Hoegfeldt, U. S. Lindholm, and A. Nagy: *Trans. ASME, J. Engng. Mats. & Tech.*, 1983, vol. 105, p. 48.
6. G. R. Johnson and U. S. Lindholm: in "Material Behavior under High Stress and Ultrahigh Loading Rates", J. Mescall and V. Weiss, eds., Plenum Press, New York, NY, 1983, p. 61.
7. T. W. Penrice: in "Powder Metallurgy in Defense Technology," *Proc. of 1979 Powder Metallurgy in Defense Technology Seminar*, Yuma, AZ, Metal Powder Industries Federation, Princeton, NJ, 1980, vol. 5, p. 11.
8. D. V. Edmonds and P. N. Jones: *Metall. Trans. A*, 1979, vol. 10A, p. 289.
9. B. C. Muddle: *Metall. Trans. A*, 1984, vol. 15A, p. 1089.
10. R. L. Woodward: *Metall. Trans. A*, 1977, vol. 8A, p. 1833.
11. U. S. Lindholm, A. Nagy, G. R. Johnson, and J. M. Hoegfeldt: *Trans. ASME J. Engng. Mats. & Tech.*, 1980, vol. 102, p. 376.
12. R. L. Woodward and R. H. Brown: *Proc. Instn. Mech. Engrs.*, 1975, vol. 189, p. 107.
13. A. Holzer: 8th North American Metalworking Research Congress, Univ. of Missouri, Rolla, MO, May 1980, *SME*, p. 110.
14. R. Papirno, J. F. Mescall, and A. M. Hansen: in "Compression Testing of Homogeneous Materials and Composites", ASTM STP 808, R. Chait and R. Papirno, eds., American Society for Testing and Materials, 1983, p. 40.
15. A. Nadai: *Theory of Flow and Fracture of Solids*, 2nd ed., McGraw-Hill, New York, NY, 1950, vol. 1, p. 309.
16. E. O. Hall: *Yield Point Phenomenon in Metals and Alloys*, Macmillan, London, 1970, p. 3.